

4

AD-A202 115

SECURITY CLASSIFICATION OF THIS PAGE (When Data Entered)

REPORT DOCUMENTATION PAGE

READ INSTRUCTIONS BEFORE COMPLETING FORM

|   |  |   |                               |
|---|--|---|-------------------------------|
| 1. REPORT NUMBER<br># 1   |  | 2. GOVT ACCESSION NO.   | 3. RECIPIENT'S CATALOG NUMBER |
| 4. TITLE (and Subtitle)<br>Effects of Annealing on the Polarization Switching of Phase I Poly(vinylidene fluoride)  |  | 5. TYPE OF REPORT & PERIOD COVERED<br>Technical Report<br>April, 1988 - December 1988 |                               |
| 7. AUTHOR(s)<br>Y. Takase, J.L. Scheinbeim and B.A. Newman  |  | 6. PERFORMING ORG. REPORT NUMBER  |                               |
| 9. PERFORMING ORGANIZATION NAME AND ADDRESS<br>Rutgers, The State University of New Jersey<br>College of Engineering, P.O. Box 909<br>Piscataway, NJ 08855-0909 |  | 8. CONTRACT OR GRANT NUMBER(s)<br>N00014-88-K-0122<br>N-88-Scheinbeim                 |                               |
| 11. CONTROLLING OFFICE NAME AND ADDRESS<br>Office of Naval Research<br>Arlington, VA 22217  |  | 10. PROGRAM ELEMENT, PROJECT, TASK AREA & WORK UNIT NUMBERS                           |                               |
| 14. MONITORING AGENCY NAME & ADDRESS (if different from Controlling Office)   |  | 12. REPORT DATE<br>December 1988  |                               |
|   |  | 13. NUMBER OF PAGES<br>26   |                               |
|   |  | 13. SECURITY CLASS. (of this report)<br>Unclassified                                  |                               |
|   |  | 13a. DECLASSIFICATION/DOWNGRADING SCHEDULE  |                               |

16. DISTRIBUTION STATEMENT (of this Report)  
 Technical report distribution list DL/1113/87/2 for unlimited distribution and release

**DTIC ELECTE**  
**S** **D**  
 JAN 03 1989  
**E**

17. DISTRIBUTION STATEMENT (of the abstract entered in Block 20, if different from Report)  
 For unlimited distribution and release

18. SUPPLEMENTARY NOTES  
 Submitted, J. Polym. Sci., Polymer Physics Ed.

19. KEY WORDS (Continue on reverse side if necessary and identify by block number)

20. ABSTRACT (Continue on reverse side if necessary and identify by block number)  
 To obtain information about microscopic processes involved in the polarization switching in uniaxially oriented poly(vinylidene fluoride) film, a least squares estimation of nonlinear parameters was developed to yield parameters of an equation which describes the nucleation and domain growth process. Time domain measurements of polarization reversal revealed that switching times decreased as the annealing temperature,  $T_a$ , increased (67.0  $\mu$ s, 52.4  $\mu$ s and 41.3  $\mu$ s at  $-20^\circ\text{C}$  under a 200 MV/m pulse field for the as-stretched samples, the samples being annealed at  $T_a = 120^\circ\text{C}$ , and  $T_a = 160^\circ\text{C}$ , respectively). The analysis

OVER

showed that the value of the domain growth speed increased as  $T_a$  increased. This is consistent with X-ray diffraction data which indicated that the annealing process brought about better chain packing and increased crystallite perfection. The analysis also showed that the nucleation probably significantly increased as  $T_a$  increased. This result was interpreted in terms of a morphological transformation, which was indicated by the decrease in elastic modulus with increasing  $T_a$  with no corresponding loss of orientation. It is suggested that the annealing process brought about an increase in the number of nucleation sites as a result of a transformation from a fibrous structure to a crystal-amorphous series structure which has increased boundary zone area.

OFFICE OF NAVAL RESEARCH

Contract ~~NA00014-88-K-0122~~ <sup>NA00014-88-K-0122</sup>

Technical Report # 1

**Effects of Annealing on the Polarization Switching of  
Phase I Poly(vinylidene fluoride)**

by

**Y. Takase, J.I. Scheinbeim and B.A. Newman**

**Rutgers University  
Department of Mechanics and Materials Science  
College of Engineering  
Piscataway, New Jersey 08855-0909**

Prepared for Publication in

**J. Poly. Sci., Poly. Phys. Ed.**

**Reproduction in whole or in part, is permitted for  
any purpose of the United States Government**

**This document has been approved for public  
release and sale; its distribution is unlimited**

**Effects of Annealing on the Polarization Switching  
of Phase I Poly(Vinylidene Fluoride)**

Y. Takase, J. I. Scheinbeim, and B. A. Newman

Department of Mechanics and Materials Science, College of  
Engineering, Rutgers University, Piscataway, New Jersey 08854

**Synopsis**

To obtain information about microscopic processes involved in the polarization switching in uniaxially oriented poly(vinylidene fluoride) film, a least squares estimation of nonlinear parameters was developed to yield parameters of an equation which describes the nucleation and domain growth process. Time domain measurements of polarization reversal revealed that switching times decreased as the annealing temperature,  $T_a$ , increased (67.0  $\mu$ s, 52.4  $\mu$ s and 41.3  $\mu$ s at  $-20^\circ\text{C}$  under a 200 MV/m pulse field for the as-stretched samples, the samples being annealed at  $T_a = 120^\circ\text{C}$ , and  $T_a = 160^\circ\text{C}$ , respectively). The analysis showed that the value of the domain growth speed increased as  $T_a$  increased. This is consistent with X-ray diffraction data which indicated that the annealing process brought about better chain packing and increased crystallite perfection. The analysis also showed that the nucleation probability significantly increased as  $T_a$  increased. This result was interpreted in terms of a morphological transformation, which was indicated by the decrease in elastic modulus with increasing  $T_a$  with no corresponding loss of orientation. It is suggested that the annealing process brought about an increase in the

number of nucleation sites as a result of a transformation from a fibrous structure to a crystal-amorphous series structure<sup>1</sup> which has increased boundary zone area.

## INTRODUCTION

Poly(vinylidene fluoride) ( $\text{PVF}_2$ ) and Poly(vinylidene fluoride-trifluoroethylene) [ $\text{P}(\text{VF}_2/\text{TrFE})$ ] copolymers are now commonly designated as ferroelectric polymers. This is because the crystalline regions of these polymers exhibit a spontaneous polarization and their polarity is reversible under the application of an electric field. In addition, ferroelectric materials commonly exhibit other characteristic features, such as paraelectric to ferroelectric phase transitions and formation of domain structures.  $\text{PVF}_2$  does not show the paraelectric to ferroelectric transition; however, the copolymer exhibits a well defined transition<sup>2</sup> and the Curie point,  $T_C$ , shifts to higher temperatures as the mole fraction,  $x$ , of  $\text{VF}_2$  increases. Extrapolation of the  $T_C$  vs  $x$ -curve to  $x = 100\%$  predicts the  $T_C$  of  $\text{PVF}_2$  to be about  $205^\circ\text{C}$ ,<sup>3</sup> which is above the melting point.

At the present, identification of domain structures remains one of the central problems in the study of polymer ferroelectrics. The main reason for this difficulty arises from the fact that many of the techniques used to observe domains in inorganic materials cannot be applied directly to polymeric materials. Domains in inorganic materials are mostly observed in single crystals.<sup>4-8</sup> In this case, the domains become large enough to be visible by employing various techniques; the colloid decoration method,<sup>4</sup> the ion adsorption and decoration method<sup>5</sup>, the dew method<sup>6</sup> and the etching method.<sup>7,8</sup> In the case of polymeric ferroelectrics, however, the crystals are much smaller (less than micron order) than inorganic single crystals.

Therefore, it is quite hard to observe domain structures in the crystalline regions. If the boundary zones between crystallites are small enough that dipole interaction still occurs, an inter-crystallite domain may be formed which could be visibly large as in liquid crystal ferroelectrics<sup>9</sup> or ceramic ferroelectrics.<sup>10</sup> To our knowledge, however, no clear observation of domain structures in polymeric ferroelectrics has been reported as yet.

Although visible observation of domain structures is quite difficult, it is known from D - E hysteresis measurements<sup>11</sup> (D is the electric displacement and E the electric field), polarization switching transient measurements<sup>12,13</sup> and X-ray diffraction studies<sup>14,15</sup> that the crystalline polarization in PVF<sub>2</sub> almost completely orients in the direction of the applied electric field and becomes a single domain from a macroscopic point of view. It is also understood from the shape of D - t curves<sup>12</sup> or J - t curves<sup>13</sup> (J being the current density and t the time) that the dipole orientation process in PVF<sub>2</sub> does not result from the independent motion of individual dipoles (a Debye type relaxation) but from the cooperative motion of dipoles.<sup>12,16</sup> Until now, most studies concerning the polarization switching mechanisms in PVF<sub>2</sub> have been devoted to describing the cooperative motion of dipoles. Dvey-Aharon et. al.<sup>17</sup> proposed a solitary-wave propagation model. Odajima et. al.<sup>18</sup> showed that the measured polarization switching characteristics of PVF<sub>2</sub> can be interpreted in terms of the nucleation and growth theory initially proposed by Wieder<sup>16</sup> for colemanite. Clark and Taylor<sup>19</sup> developed their solitary-wave model<sup>17</sup> of ferroelectric switching to allow comparison with switching measurements.<sup>12</sup> Furukawa et.

al.<sup>20</sup> discussed the shape of switching transients for PVF<sub>2</sub> on the basis of a nucleation and growth model.<sup>16</sup> They showed that the model is consistent with experimental observations if one-dimensional growth and an appropriate ratio of growth velocity to nucleation probability are assumed. Takase et. al.<sup>21</sup> developed their nucleation and domain growth model<sup>18</sup> on the basis of a close examination of the analytical results; that the previous theory<sup>18,20</sup> can only account for the switching characteristic of PVF<sub>2</sub> in the time zone in which the majority of switching (~ 40 % of the total switching charge) takes place. Their modification is based on the idea that all nucleation is not necessarily followed by domain growth but that some nuclei may remain as fixed (small) size domains or as microdomains. They obtained parameters of an equation which describes their modified nucleation and domain growth model by employing mathematical curve fitting techniques: a least squares estimation of the nonlinear parameters resulting from their model.

The determination of these parameters is quite important because it provides information about the microscopic process of polarization reversal, while the conventional switching time approach only characterizes the macroscopic phenomenon. In a previous paper,<sup>21</sup> one of the authors showed the results of their analysis applied to the data from measurements of the temperature dependence of the switching characteristics of PVF<sub>2</sub>. In the present paper, we hope to show a detailed analytical procedure for obtaining a least squares estimation of the nonlinear parameters which is generally applied to the switching transient



characteristics (J - t curves) of PVF<sub>2</sub> and of several P(VF<sub>2</sub>/TrFE) copolymers. This time, the effect of annealing on the switching characteristics has been analyzed and discussed in connection with the data obtained by X-ray diffraction, dielectric constant and elastic modulus measurements.

### ANALYTICAL METHOD

#### Modified Nucleation and Domain Growth Model

First, the modified nucleation and growth model<sup>21</sup> for ferroelectric switching in PVF<sub>2</sub> is reviewed briefly. In this model, the volume fraction of a polarization domain, X', that has been transformed (or switched) by formation and growth of (fictitious) nuclei, without mutual impingement, is expressed as:

$$X' = \int_0^t [\pi v^2 l (t-\tau)^2 \dot{N}_1(\tau) + V_0 \dot{N}_2(\tau)] d\tau. \quad (1)$$

The first term in the integrand represents the main switching process and involves the usual random nucleation at a rate of  $\dot{N}_1(\tau) = N_0 \nu \exp(-\nu\tau)$  followed by two-dimensional growth in a crystalline region with a thickness  $l$  at a constant speed  $v$ ;  $N_0$  being the total number of nucleation sites per unit volume, and  $\nu$  the nucleation probability. The second term in the integrand represents the formation of microdomains per unit volume at a rate of  $\dot{N}_2(\tau)$  and assumes no further growth of these domains. The microdomains are each assumed to have the same volume,  $V_0$ .

The actual volume fraction, X, that has undergone transformation at time t is related to X' by  $dX/dX' = 1 - X$ .<sup>22</sup>

Consequently, if we assume the charge due to polarization reversal,  $D$ , to be proportional to the transformed volume fraction  $X$ , then:

$$D = D_0[1 - \exp(X')], \quad (2)$$

where  $D_0 = D(\infty)$ .

Equation (1) contains the function  $\dot{N}_2(\tau)$  whose explicit form cannot be given directly on the basis of the nucleation concept. However, because the current density,  $J$ , is related to  $D$  by  $J = dD/dt$  and the  $J - t$  curves can be described by a power law in  $t$ ,<sup>23</sup> we assume the function  $\dot{N}_2$  to be of the following form:

$$V_0 \dot{N}_2(\tau) = V_0(1 + \nu_1 \tau)^{-m} = f_1, \quad (3)$$

where  $\nu_0 = V_0 \dot{N}_2(0)$  is the volume of microdomains which reorient at  $\tau = 0$  per unit time per unit volume,  $m$  is a positive constant.  $\nu_1$  is chosen to be  $10^{10}$  Hz as was done previously.<sup>21</sup>

Substituting Eq. (2) into Eq. (1) and noting again that  $J(t) = dD/dt$ , we obtain

$$J(t) = D_0 \left( \frac{2G^2}{\nu} (e^{-\nu t} - \sum_{p=0}^{\infty} \frac{(-\nu t)^p}{p!}) + f_1 \right) \times \exp \left( \frac{2G^2}{\nu^2} (e^{-\nu t} - \sum_{p=0}^{\infty} \frac{(-\nu t)^p}{p!}) - f_2 \right), \quad (4)$$

where  $G = v(\pi N_0 \ell)^{1/2}$  is proportional to the growth speed during the main switching process and

$$f_2 = \nu_0 [(1 + \nu_1 t)^{1-m} - 1] / [\nu_1 (1-m)] \text{ if } m \neq 1.$$

Equation (4) contains five parameters  $D_0$ ,  $G$ ,  $\nu$ ,  $\nu_0$ , and  $m$  which can be adjusted to achieve a close fit between the equation and the  $J - t$  curves using a least squares estimation of nonlinear parameters.

#### Least Square Estimation of the Five Nonlinear Parameters

According to the present model, the relation between variables  $J$  and  $t$  is expressed by eq. (4) which has the general form:

$$J = f(t, c_1, c_2, c_3, c_4, c_5), \quad (5)$$

where  $c_1, \dots, c_5$  are five unknown independent parameters. They are found in eq. (4) as nonlinear parameters. The switching measurements yield sets of data  $(J_i, t_i)$  ( $i=1$  to  $n$ ) for different values,  $t_i$ , of the independent variable  $t$ . If we can obtain estimated values for the parameters,  $c_1^0, \dots, c_5^0$ , which are close to their real values, the "calculation" error,<sup>24</sup>

$$R_i = f(t_i, c_1^0, \dots, c_5^0) - J_i, \quad (i = 1 \text{ to } n), \quad (6)$$

can be obtained.

Expanding equation (5) as a Taylor series about  $(c_1^0, \dots, c_5^0)$ , the relation between the "true" error,  $r_i$ , and the "calculation" error,  $R_i$ , we obtain<sup>24</sup>

$$r_i = R_i + \frac{\partial f_i}{\partial c_1} \delta c_1 + \dots + \frac{\partial f_i}{\partial c_5} \delta c_5, \quad (i = 1 \text{ to } n). \quad (6)$$

As is usual in the case of a least squares estimation method, the sum of squares of the "true" error,

$$\sum_{i=1}^n r_i^2 = \sum_{i=1}^n [R_i + \frac{\partial f_i}{\partial c_1} \delta c_1 + \dots + \frac{\partial f_i}{\partial c_5} \delta c_5]^2, \quad (7)$$

should be minimized. This procedure is carried out by solving the normal equation expressed as<sup>24</sup>

$$\begin{pmatrix} a_{11} & a_{12} & a_{13} & a_{14} & a_{15} \\ a_{21} & a_{22} & a_{23} & a_{24} & a_{25} \\ a_{31} & a_{32} & a_{33} & a_{34} & a_{35} \\ a_{41} & a_{42} & a_{43} & a_{44} & a_{45} \\ a_{51} & a_{52} & a_{53} & a_{54} & a_{55} \end{pmatrix} \begin{pmatrix} \delta c_1 \\ \delta c_2 \\ \delta c_3 \\ \delta c_4 \\ \delta c_5 \end{pmatrix} = \begin{pmatrix} b_1 \\ b_2 \\ b_3 \\ b_4 \\ b_5 \end{pmatrix} \quad (8)$$

where

$$a_{jk} = \sum_{i=1}^n \left( \frac{\partial J_i}{\partial c_j} \frac{\partial J_i}{\partial c_k} \right), \quad (j=1 \text{ to } 5, k=1 \text{ to } 5), \quad (9)$$

$$b_j = - \sum_{i=1}^n \left( \frac{\partial J_i}{\partial c_j} R_i \right), \quad (j=1 \text{ to } 5).$$

If we put  $c_1 = D_0$ ,  $c_2 = G$ ,  $c_3 = \nu$ ,  $c_4 = \nu_0$  and  $c_5 = m$ , we can calculate each derivative in the matrix element to be:

$$\begin{aligned} \frac{\partial J}{\partial c_1} &= \frac{\partial J}{\partial D_0} = J(t)/D_0, \\ \frac{\partial J}{\partial c_2} &= \frac{\partial J}{\partial G} = 4G[D_0 g_2 g_4 + J(t) g_3 / \nu] / \nu, \\ \frac{\partial J}{\partial c_3} &= \frac{\partial J}{\partial \nu} = -2(G/\nu)^2 [D_0 (\nu t g_1 + g_2) g_4 + J(t) (\nu t g_2 + 2g_3) / \nu], \\ \frac{\partial J}{\partial c_4} &= \frac{\partial J}{\partial \nu_0} = D_0 g_4 g_6 - J(t) f_2 / \nu_0, \\ \frac{\partial J}{\partial c_5} &= \frac{\partial J}{\partial m} = -D_0 \nu_0 g_4 g_6 g_7 - J(t) (f_2 - \nu_0 g_5 g_6 g_7 / \nu_1) / (1-m), \end{aligned} \quad (10)$$

where

$$\begin{aligned}g_1 &= e^{-vt} - 1, \\g_2 &= g_1 + vt, \\g_3 &= g_2 - (vt)^2/2, \\g_4 &= \exp[2(G/V)^2 g_3] - f_2, \\g_5 &= 1 + V_1 t, \\g_6 &= g_5^{-m}, \\g_7 &= \ln(g_5).\end{aligned}\tag{11}$$

Usually, either an iterative method or a direct method is used to solve Eq. (5). In the present case, the direct method (or the Gauss-Jordan elimination) was effective and accurate enough to be applied. The solution of the normal equation ( $\delta c_1, \delta c_2, \dots, \delta c_5$ ) gives the first order approximation of the small correction of the initial values ( $c^0_1, c^0_2, \dots, c^0_5$ ). If  $|\delta c_k/c_k| > \Delta$ ,  $\Delta$  being a small positive number, the initial values should be replaced by  $c^0_j + \delta c_j$  ( $j = 1$  to  $5$ ) and the calculation repeated iteratively.

#### EXPERIMENTAL

Samples used in this study were 7- $\mu$ m-thick uniaxially oriented PVF<sub>2</sub> films (KF1000) supplied by Kureha Chemical Industry, Co., Ltd. Annealed samples were prepared by heat treatment in nitrogen gas at 100, 120, 140 and 160°C for 2 hours. During heat treatment, films were mechanically fixed to prevent shrinkage.

Gold electrodes, each about 2.5  $\times$  5 mm<sup>2</sup> in area, were

deposited on opposing surfaces of the films by vacuum evaporation.

All measurements, except X-ray measurements, were carried out by placing the sample in an electrically shielded copper cell equipped with heater and temperature sensors.

X-ray diffraction profiles were obtained at room temperature using a Philips XRG 3100 X-ray generator, and  $\text{CuK}\alpha$  radiation, filtered with a Ni foil.

The time domain characteristics of polarization switching were measured at  $-20^{\circ}\text{C}$  using a high voltage power supply equipped with an SCR switch and a digital waveform recorder (Tektronics 390 AD). The switching time of the SCR switch is about 1  $\mu\text{s}$ .

The dielectric constant and elastic modulus were measured by using a Rheograph Solid <sup>®</sup> (Toyoseiki, Japan). The frequency of the excitation signal was 10 Hz.

Operation of various functions in the system was consigned to a microcomputer (IBM-XT) which also performed the task of data processing.

## RESULTS AND DISCUSSION

The switching current density,  $J$ , of the as-stretched samples and samples annealed at  $T_a = 120$  and  $160^{\circ}\text{C}$  was measured at  $-20^{\circ}\text{C}$  by applying a rectangular electric field pulse of 200 MV/m, and is shown in Figure 1. This data is the steady state switching behavior obtained after 40 switching cycles. The least squares estimation was applied to the data and the results are shown in the same figure. Agreement between theory (dotted lines)

and experiment (solid lines) is excellent in the time region where the initial and the main switching of dipoles<sup>21</sup> are almost completed. After the main switching, the measured current does not decay rapidly. Since this component does not significantly contribute to the total switching charge, the present model neglects it. However, for some practical purposes, such as determining the switching time, this component causes difficulties. Until now, the switching time of the polarization reversal of PVF<sub>2</sub> has not been determined in the usual manner but has instead been identified in a special manner; the time where the quantity  $\partial D/\partial \log t$  peaks.<sup>20</sup> Since eq. (4) does not include this kind of component but fits the measured data, it is reasonable to determine the switching time of the sample by applying a more universal definition (the time when the phenomenon reaches 90 % of the steady state value) to the theoretical curve instead of the measured curve.

Theoretical  $D/D_0 - t$  curves corresponding to the three  $J - t$  curves in Figure 1 are shown in Figure 2. The switching times are indicated by a "+" mark. They are 67.0, 52.4, and 41.3  $\mu$ s for the as-stretched sample, the sample annealed at 120°C and the sample annealed at 160°C, respectively. The switching time significantly decreases as the annealing temperature increases; from 67.0  $\mu$ s (as-stretched sample) to 52.4  $\mu$ s ( $T_a = 120^\circ\text{C}$ ), a change of -21.8 % and to 41.3  $\mu$ s ( $T_a = 160^\circ\text{C}$ ), a change of -38.4 %. These changes appear to result from the changes in microstructure apparent in the X-ray data (see Fig. 4); the data shows that the half width changes from 1.52° (as-stretched sample) to 1.39° ( $T_a = 120^\circ\text{C}$ ), a change of -8.55 % and to 1.09° ( $T_a = 160^\circ\text{C}$ ), a change of

-28.3 %. This is indicative of the dependence of the polarization reversal process on microstructure as is usual for a domain growth process.<sup>18</sup>

The three physically important parameters,  $G$ ,  $\nu$ , and  $\nu_0$ , determined from the present analysis are shown in Figure 3 as a function of annealing temperature. Both values of the domain growth speed (which is proportional to  $G$ ) and the nucleation probability,  $\nu$ , increase as the annealing temperature increases. In contrast to  $G$  and  $\nu$ , the value of  $\nu_0$  (the microdomain nucleation probability) decreases as the annealing temperature increases.

Figure 4 shows the  $2\theta$ -values and half width,  $\beta_{1/2}$ , for the composite (110)(200) reflection of the phase I crystal form as a function of annealing temperature. The  $2\theta$ -value increases monotonically as the annealing temperature,  $T_a$ , increases, while the half width decreases monotonically as  $T_a$  increases. These results indicate that the annealing process brings about better chain packing and increased crystallite perfection. Given the dependence of  $G$  and  $\beta_{1/2}$  on  $T_a$ , it is quite reasonable to assume that the domain growth speed increases in the crystalline regions because there are less defects.

Figure 5 shows the real part of the dielectric constant,  $\epsilon'$ , the elastic modulus,  $c'$ , and the polarization,  $P_r$ , as a function of annealing temperature. The values of  $\epsilon'$  and  $c'$  decrease as the annealing temperature increases from 100 to 160°C, while the value of  $P_r$  remains almost constant ( $\sim 56 \text{ mC/m}^2$ ). The annealing temperature dependence of  $\epsilon'$  and  $c'$  resemble each other. It is



difficult to include their observed annealing effects in the idealized models of PVF<sub>2</sub> where lamellar crystallites are distributed in an amorphous matrix.<sup>25,26</sup> The decrease in dielectric constant at a temperature well above the glass transition point might be attributed to an increase in crystallinity, but this would be inconsistent with the observed decrease in modulus with annealing temperature. If we assume that annealing brings about increased tension on the molecular chains in the amorphous regions, the elastic modulus should increase. This is also opposite to what we observe in the annealing temperature dependence of the modulus.

In order to solve this difficulty, we have proposed a model<sup>27</sup> which allows a morphological transformation.<sup>1</sup> Since the present film is drawn at 100°C by roller to about five times the original length, the plastic deformation has, to some extent, destroyed the stacks of thin and wide parallel lamellae present in the starting material and has transformed them into a fibrous structure. Therefore, the elastic properties of the film may be understood by a parallel connection of essentially two elements; one is a series connection of folded chain crystallites and amorphous regions and the other is a continuous fibrous structure. The elastic modulus of the drawn fibrous structure strongly depends on the draw ratio and has a high value of up to 50 % of that of the ideal crystal lattice in the chain direction,  $c_c$ , while an isotropic lamellar material has a value about 0.01  $c_c$ .<sup>1</sup> The as-stretched film consists of a large fraction of fibrous structure. If a sample is annealed at high temperature, a part of the fibrous structure can transform to folded chain

crystallites which show better packing of molecular chains. As the modulus of the folded chain crystal structure is less than the modulus of the fibrous structure, the transformation brings about a decrease in bulk modulus. The significant increase in nucleation probability is considered to be directly related to this transformation; as a result of the transformation, the number of folded chain crystallites increases and, consequently, their boundary zones adjacent to the amorphous regions increase in size. According to the nucleation and domain growth model, the boundary zones are assumed to be the sites where nucleation occurs.

The decrease in the microdomain nucleation probability,  $\nu_0$ , implies that the orientation of microdomains per unit time decreased or that more nucleation sites are present to allow domain growth, since the total polarization is almost constant for all of the samples (see Fig. 5). This is also reasonable since the crystalline regions and amorphous regions are more distinct as a result of the transformation from fibrous to folded chain crystals.

We have applied the present least squares estimation method not only to annealed samples but also to samples treated under other conditions. Some of them are as-stretched PVF<sub>2</sub> films,  $\gamma$ -ray irradiated PVF<sub>2</sub> films, as-cast 72/28 mol % P(VF<sub>2</sub>/TrFE) films and  $\gamma$ -ray irradiated 72/28 mol % P(VF<sub>2</sub>/TrFE) films at temperatures from -80 to 20 °C. The results indicate that the present method is applicable to all types of samples, provided proper initial values of the five parameters are used. Therefore, to find the

initial values of these parameters is of prime importance. A program based on a simple iterative method to find the least squares of errors is usually quite useful for order estimation of these parameters, since the values of  $G$ ,  $\nu$ , and  $\nu_0$  range over several orders, depending on sample condition. An example for the sample annealed at  $160^\circ\text{C}$  is given in Tables I and II. When the present method is applied to the data of the 7 sampling points listed in Table I and the set of initial values of parameters listed in Table II are chosen, the final solution is obtained after the 10th iteration when the value of  $\Delta$  equals  $10^{-6}$ .

It is interesting to note that the  $\gamma$ -ray irradiation brings about the opposite effect of annealing; suppression of the nucleation probability.<sup>21</sup> The results of the analysis of the annealing and  $\gamma$ -ray irradiation on the nucleation and domain growth process are physically quite reasonable. Therefore, we believe that our experimental results using our model and analysis have yielded further insights into the microscopic process of the polarization switching mechanism in  $\text{PVF}_2$  films.

#### CONCLUSIONS

The switching time decreases as the annealing temperature,  $T_a$ , increases (e. g. 67.0, 52.4 and 41.3  $\mu\text{s}$  at  $-20^\circ\text{C}$  under a 200 MV/m electric field for the as-stretched sample, and samples annealed at  $T_a = 120^\circ\text{C}$  and  $160^\circ\text{C}$ , respectively).

The five independent parameters in the equation which describes the nucleation and domain growth process can be obtained by a least squares estimation of these nonlinear

parameters.

Analysis shows that the value of the domain growth speed increases as  $T_a$  increases. This result, combined with the X-ray diffraction data, implies that better chain packing and increased crystallite perfection results in increased domain growth speed.

The analysis also shows that the nucleation probability significantly increases as  $T_a$  increases. This is interpreted in terms of a morphological transformation, which is suggested by a decrease in elastic modulus with increasing  $T_a$ . The annealing brings about increased nucleation sites as a result of the transformation from a fibrous structure to a folded chain crystal structures which has increased boundary zone area.

The present model and analysis have been shown to yield physically reasonable results for the microscopic parameters which describe the polarization reversal in  $PVF_2$  films for phenomena which enhance and delay the switching time.

#### ACKNOWLEDGMENT

This work was supported by the Office of Naval Research.

## References

1. A. Peterlin, *J. Appl. Phys.* **48**, 4099 (1977).
2. T. Furukawa, M. Date, E. Fukada, Y. Tajitsu, and A. Chiba, *Jpn. J. Appl. Phys.* **19**, L109 (1980).
3. A. J. Lovinger, T. Furukawa, G. T. Davis, and M. G. Broadhurst, *Polymer* **24**, 1233 (1983).
4. G. L. Pearson and W. L. Feldmann, *J. Phys. Chem. Solids* **9**, 28 (1959).
5. A. Sawada and R. Abe, *Jpn. J. Appl. Phys.* **5**, 401 (1966).
6. S. D. Toshev, *Kristallografiya* **8**, 114, (1963), **8**, 680 (1963).
7. J. A. Hooton and W. J. Merz, *Phys. Rev.* **98**, 409 (1955).
8. H. L. Stadler and P. J. Zachmanidis, *J. Appl. Phys.* **34**, 3255 (1963), **35**, 2895 (1964).
9. H. Takezoe, Y. Ouchi, K. Ishikawa and A. Fukuda, *Mol. Cryst. Liq. Cryst.* **139**, 27 (1986).
10. D. Berlincourt and H. H. A. Krueger, *J. Appl. Phys.* **30**, 1804 (1959).
11. M. Tamura, K. Ogasawara, N. Ono, and S. Hagiwara, *J. Appl. Phys.* **45**, 3768 (1974).
12. T. Furukawa and G. E. Johnson, *Appl. Phys. Lett.* **38**, 1027 (1981).
13. Y. Takase and A. Odajima, *Jpn. J. Appl. Phys.* **21**, L707 (1982).
14. R. G. Kepler and R. A. Anderson, *J. Appl. Phys.* **49**, 1232 (1978).
15. N. Takahashi and A. Odajima, *Ferroelectrics*, **32**, 49 (1981).
16. H. H. Wieder, *J. Appl. Phys.* **31**, 180 (1960).

17. H. Dvey-Aharon, T. J. Sluckin, and P. L. Taylor, Phys. Rev. B21, 3700 (1980).
18. A. Odajima, Y. Takase, and N. Takahashi, Proc. Inst. Electrostat. Jpn. 5, 312 (1981) (in Japanese).
19. J. D. Clark and P. L. Taylor, Phys. Rev. Letters 49, 1532 (1982).
20. T. Furukawa and M. Date, and G. E. Johnson, J. Appl. Phys. 54, 1540 (1983).
21. Y. Takase, A. Odajima, and T. T. Wang, J. Appl. Phys. 60, 2920 (1986).
22. M. Avrami, J. Chem. Phys. 8, 212 (1940).
23. A. K. Jonscher, Nature 256, 566 (1975).
24. T. R. McCalla, "Introduction to Numerical Methods and FORTRAN Programming", chapter 8.3, John Wiley & Sons, Inc. 1967.
25. M. G. Broadhurst, G. T. Davis, and J. E. McKinney, J. Appl. Phys. 49, 4992 (1978).
26. Y. Wada and R. Hayakawa, Ferroelectrics 32, 115 (1981).
27. Y. Takase, J. I. Scheinbeim, and B. A. Newman, (submitted to J. Polymer Sci. Polymer Phy. Ed.)

Table I Sampled data of  $(t_i, J_i)$  of the switching transient for the film annealed at 160°C.

| i                              | 1    | 2    | 3    | 4    | 5    | 6    | 7    |
|--------------------------------|------|------|------|------|------|------|------|
| time ( $\mu$ s)                | 4    | 8    | 13   | 18   | 23   | 28   | 33   |
| Current density<br>( $A/m^2$ ) | 3378 | 3246 | 3260 | 3135 | 2830 | 2400 | 1914 |

Table II Initial values of the five parameters in eq. (4) and the solved values of them by the least squares estimation of nonlinear parameters when it is applied to the data in Table I.

| parameter        | $D_0$<br>( $mC/m^2$ ) | $G$<br>(Hz)         | $\nu$<br>(Hz)       | $\nu_0$<br>(Hz)     | $m$    |
|------------------|-----------------------|---------------------|---------------------|---------------------|--------|
| initial value    | 129.0                 | $3.2 \times 10^4$   | $3.7 \times 10^5$   | $4.0 \times 10^5$   | 0.26   |
| calculated value | 126.6                 | $3.106 \times 10^4$ | $3.098 \times 10^5$ | $2.393 \times 10^5$ | 0.2042 |

### Figure captions

Fig. 1. The switching current density,  $J$  of the as-stretched sample and annealed (at 120 and 160°C) samples, measured at -20°C under an electric field pulse of 200 MV/m. The dotted line and the solid line represent experimental and theoretical curves, respectively.

Fig. 2. Theoretical curves of the normalized electric displacement,  $D/D_0$ , as a function of time,  $t$ ; (1) as-stretched, (2) annealed at 120°C, and (3) annealed at 160°C corresponding to the three  $J - t$  curves in Figure 1.

Fig. 3. (a)  $G$  (proportional to the domain growth speed) vs annealing temperature,  $T_a$ . (b)  $\nu$  (nucleation probability) vs annealing temperature,  $T_a$ . (c)  $\nu_0$  (nucleation probability of microdomains) vs annealing temperature,  $T_a$ .

Fig. 4. The  $2\theta$ -values and half width,  $\beta_{1/2}$ , for the composite (110)(200) reflection of the phase I crystal form as a function of annealing temperature.

Fig. 5. (a) The real part of the dielectric constant,  $\epsilon'$ , vs the annealing temperature,  $T_a$ . (b) The elastic modulus,  $c'$ , vs the annealing temperature,  $T_a$ . (c) The polarization,  $P_r$ , vs the annealing temperature,  $T_a$ .



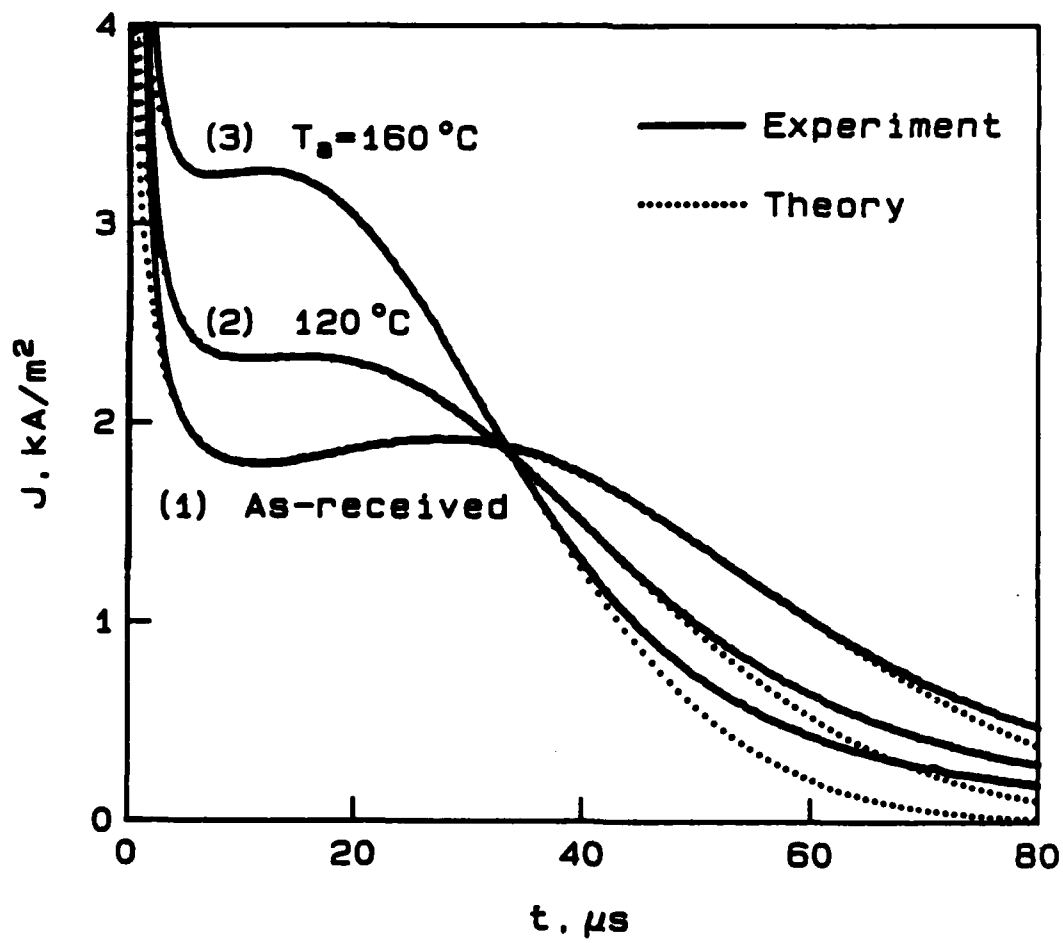


Fig. 1.

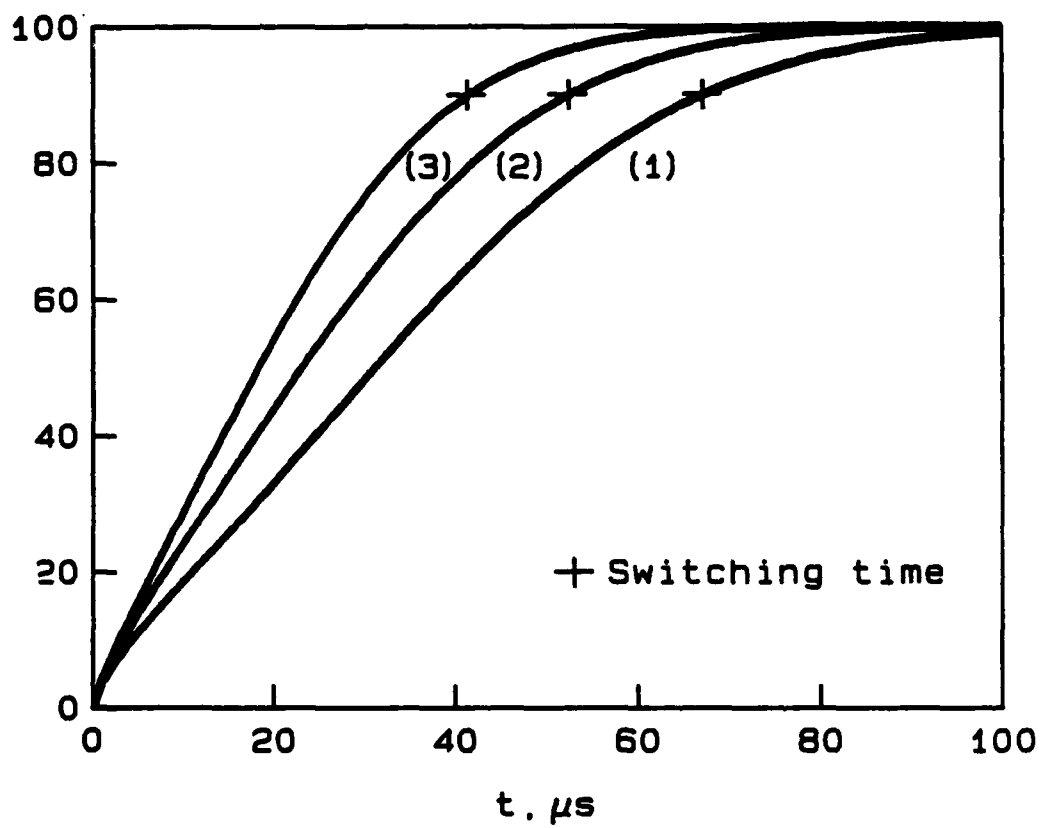


Fig. 2.

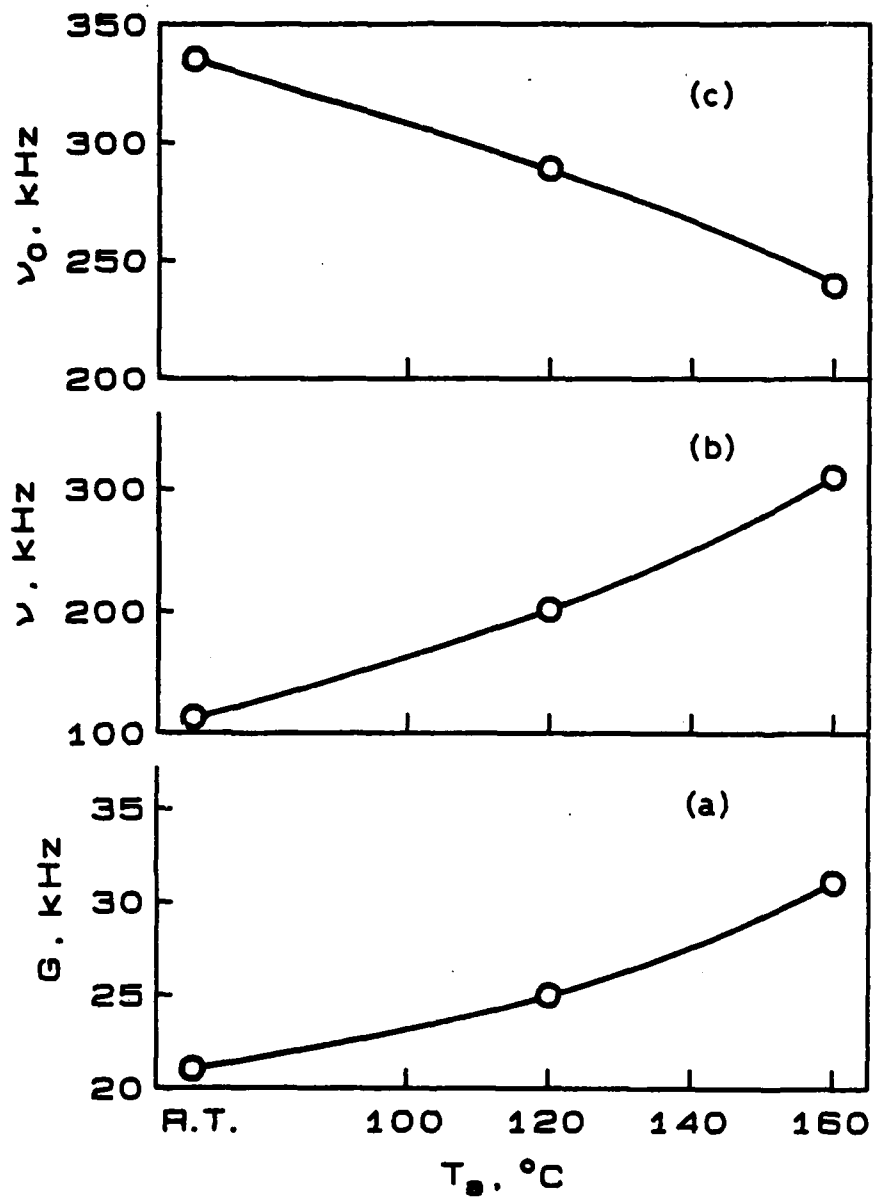


Fig. 3.

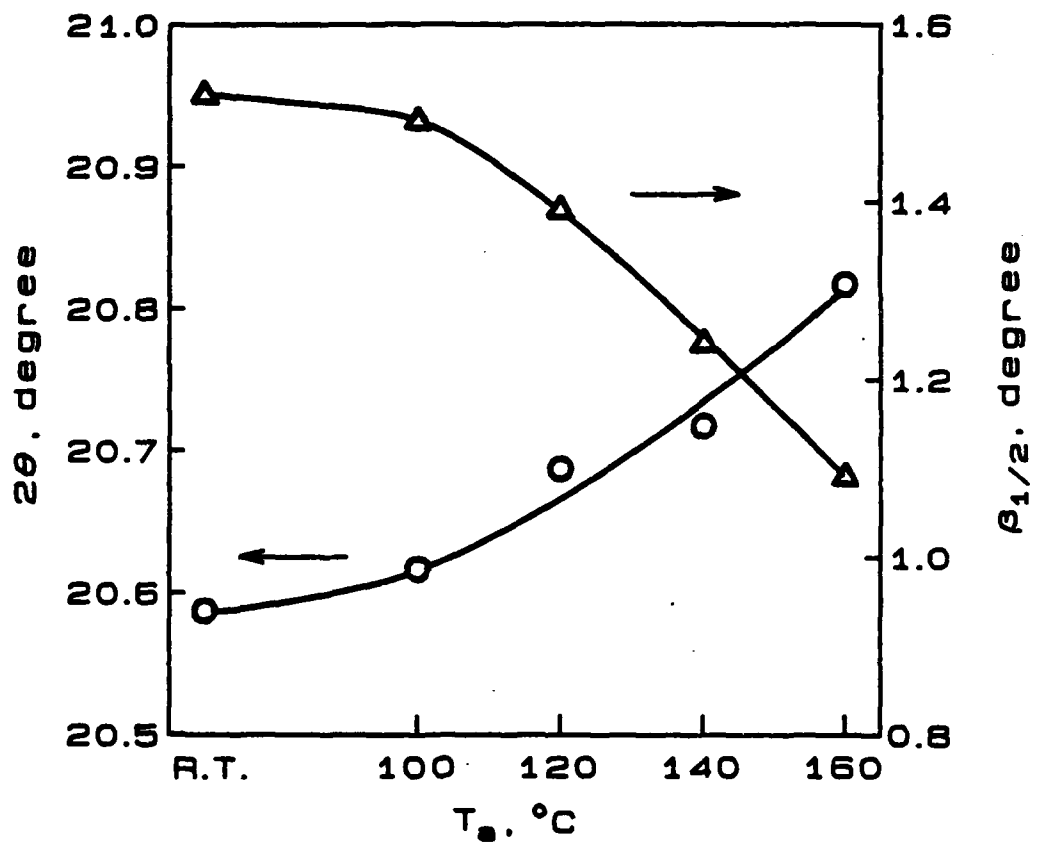


Fig. 4.

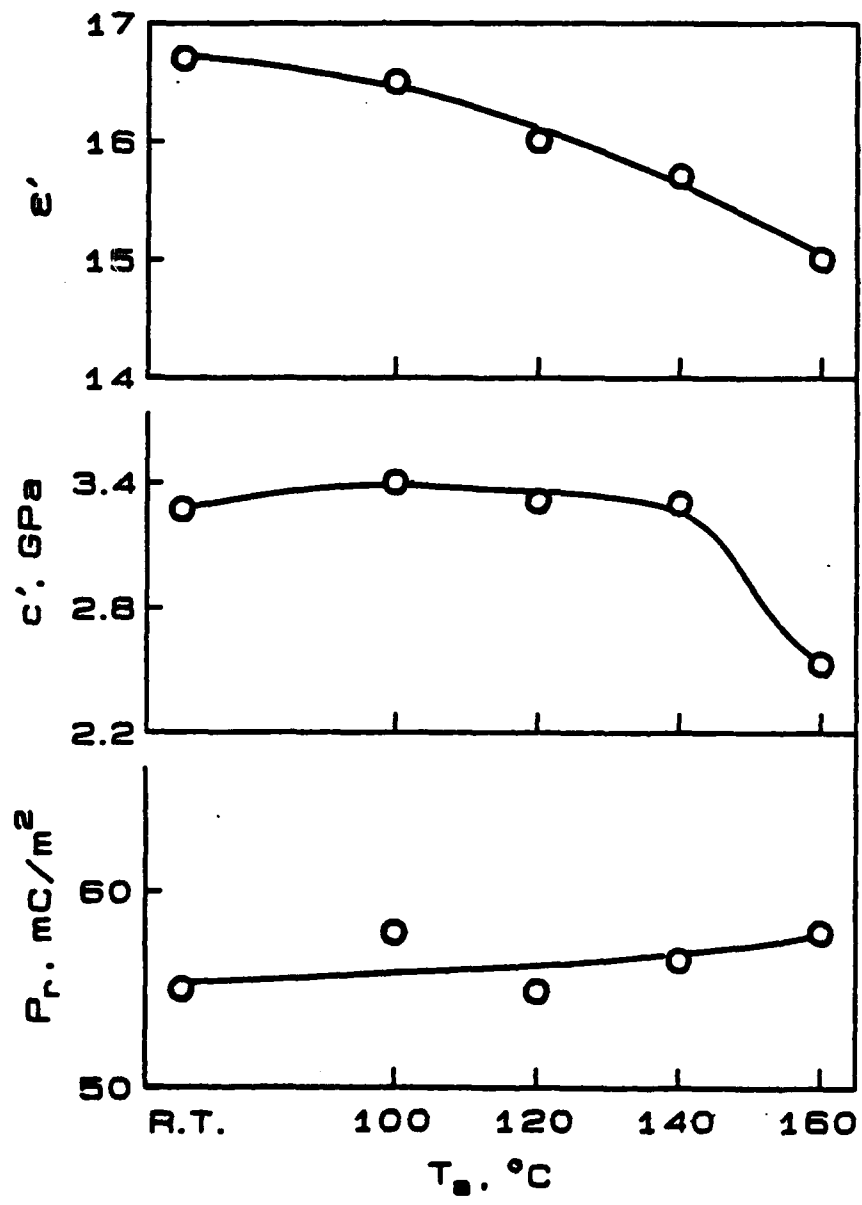


Fig. 5.